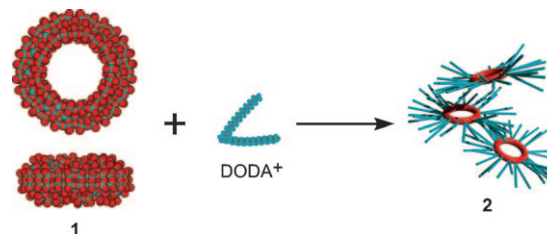


# Adsorption and Catalytic Properties of the Inner Nanospace of a Gigantic Ring-Shaped Polyoxometalate Cluster\*\*

Shin-ichiro Noro,\* Ryo Tsunashima, Yuichi Kamiya, Kazuhiro Uemura, Hidetoshi Kita, Leroy Cronin,\* Tomoyuki Akutagawa, and Takayoshi Nakamura\*

Porous materials with structurally well-defined nanoscale cavities (e.g., carbon nanostructures, zeolites, mesoporous silica, and coordination compounds)<sup>[1–3]</sup> are of great interest because of their unique properties such as adsorption, separation, exchange, and catalysis, which are all associated with the presence of a functional nanospace. In this respect, polyoxometalate clusters, which are nanosized metal-oxide macroanions built from molecular precursors with a range of unique redox and acidic properties, are ideally suited for the development of functional nanospaces but have not yet been thus explored.<sup>[4–6]</sup> Indeed, ring-shaped POMs have a great deal of potential for allowing creation of an exceptionally well defined and accessible nanosurfaces and nanospaces. These ring clusters date back to 1995, when the synthesis and structural analysis of gigantic mixed-valent ring-shaped POM cluster  $(\text{NH}_4)_{28}[\text{Mo}_{154}(\text{NO})_{14}\text{O}_{448}\text{H}_{14}(\text{H}_2\text{O})_{70}]$  ( $\{\text{Mo}_{154}\}$  ring) was first reported by Müller et al.,<sup>[5a]</sup> and later this was followed by a much more facile synthesis of the analogous compound  $\text{Na}_{14}[\text{Mo}_{154}\text{O}_{462}\text{H}_{14}(\text{H}_2\text{O})_{70}] \cdot 400\text{H}_2\text{O}$  (**1**, Scheme 1,<sup>[5b–d]</sup> for further information on ring properties, see Ref. [5f–j]) The diameter of the POM ring and inner void space are about 3.9 and 1.7 nm, respectively, while the height of ring is about 1.8 nm.<sup>[7]</sup> Despite the great potential of ring-shaped POMs to form porous materials, POM clusters have



Scheme 1. Protection of  $\{\text{Mo}_{154}\}$  ring by DODA cations.

been greatly under-utilized and -investigated, probably due to poor stability.<sup>[8]</sup>

Because of this fundamental limitation, we opted to examine the stability and functionality of a  $\{\text{Mo}_{154}\}$  ring encapsulated by dimethyldioctadecylammonium (DODA) cations (Scheme 1), because the DODA cation, with a length of about 2.5 nm, introduces amphiphilic-like properties into the POM–cation hybrid, and POM–DODA hybrids have shown some interesting properties, for example, for formation of Langmuir–Blodgett films.<sup>[9,10]</sup> Further, we hypothesized that encapsulation by DODA will also help to increase the stability of the nanoscale wheel cluster. Not only will nanoscale molecular assembly of the hybrid material be controlled by electrostatic interactions between the  $\{\text{Mo}_{154}\}$ -ring polyanion and DODA cations, hydrophobic interactions between the alkyl chains should contribute to stabilization of the hybrid material in the solid state. As reported previously,<sup>[9]</sup> the POM–DODA hybrid shows high stability in  $\text{CHCl}_3$  solution, while the ring structure of **1** is not robust in aqueous solution and the solid state (see Figures S1–S4, Supporting Information).

Here we report on the inner nanospace functionality of POM–DODA hybrid  $(\text{DODA})_{25}[\text{Mo}_{154}\text{O}_{462}\text{H}_5] \cdot n\text{H}_2\text{O}$  (**2**).<sup>[11]</sup> Initially, dynamic light scattering (DLS) experiments were conducted to confirm the presence of the  $\{\text{Mo}_{154}\}$  ring of **2** in solution and showed that the particle diameter in a solution in THF is about  $(4.0 \pm 0.6)$  nm, similar to the size of the  $\{\text{Mo}_{154}\}$  ring (Figure S5, Supporting Information). Hence, these data are consistent with the hypothesis that the  $\{\text{Mo}_{154}\}$  ring is stabilized after reaction of **1** with DODA, whereby the DODA cations effectively encapsulate the outer part of the ring, as shown in Scheme 1. Thermogravimetric analysis of **2** shows a weight loss of 4.7% in the temperature range from 298 to 440 K (Figure S6, Supporting Information), which corresponds to about 95  $\text{H}_2\text{O}$  molecules. To confirm removal of all  $\text{H}_2\text{O}$  molecules, the temperature dependence of the IR spectrum was measured. The OH stretching and OH bending bands at 3400 and 1620  $\text{cm}^{-1}$ , respectively, are observed at

[\*] Dr. S.-i. Noro, Dr. R. Tsunashima, Prof. T. Akutagawa, Prof. T. Nakamura  
 Research Institute for Electronic Science, Hokkaido University  
 Sapporo 001-0020 (Japan)  
 Fax: (+81) 11-706-9420  
 E-mail: snoro@es.hokudai.ac.jp  
 tnaka@es.hokudai.ac.jp

Prof. L. Cronin  
 WestCHEM, Department of Chemistry, University of Glasgow  
 Glasgow G12 8QQ, Scotland (UK)  
 Fax: (+44) 141-330-4888  
 E-mail: l.cronin@chem.gla.ac.uk  
 Homepage: <http://www.croninlab.com>

Prof. Y. Kamiya  
 Research Faculty of Environmental Earth Science  
 Hokkaido University  
 Sapporo 060-0812 (Japan)  
 Dr. K. Uemura, Prof. H. Kita  
 Graduate School of Science and Engineering, Yamaguchi University  
 Yamaguchi 755-8611 (Japan)

[\*\*] This work was partly supported by a Grant-in-Aid for Science Research from the Ministries of Education, Culture, Sports, Science and Technology of Japan.

Supporting information for this article is available on the WWW under <http://dx.doi.org/10.1002/anie.200903142>.

room temperature. As the temperature increases, the intensity of these bands decreases (Figures S7 and S8, Supporting Information). At 433 K, these bands almost disappear, that is, all H<sub>2</sub>O molecules are removed from **2**. On the other hand, bands due to the DODA cation and the POM ring scarcely change. The UV spectra of **2** before and after removal of all H<sub>2</sub>O in CHCl<sub>3</sub> solution are similar to each other (Figure S9, Supporting Information). These results suggest that removal of all H<sub>2</sub>O molecules has little influence on the ring structure of **2**. The irregular assembly of the ring-shaped POMs, as shown in Scheme 1, was confirmed by XRD patterns, in which only some of the broad peaks of **2** were identifiable (Figure S10, Supporting Information), and this gives a very interesting perspective for future design of these architectures, since a regular assembly of POMs with designed (e.g., rigid) cations has potential to give access to a more prominent nanospace.

In the case of hybrid **2**, it is important whether the DODA cations are located inside or outside the {Mo<sub>154</sub>} ring. The <sup>1</sup>H NMR spectra of **2** in CDCl<sub>3</sub><sup>[9]</sup> indicate that the electrostatic interaction between the negatively charged {Mo<sub>154</sub>} ring and positively charged nitrogen atom of DODA reduces the motional freedom of the head group of the DODA cation, and the relatively large thermal motions of the two octadecyl chains of DODA cations are maintained. In addition, the observation that **2** is highly soluble in nonpolar solvents such as toluene, CH<sub>2</sub>Cl<sub>2</sub>, and CHCl<sub>3</sub>, as well as the fact that the DODA cation is considerably larger than the inner space of the wheel, indicates that the DODA cations are predominantly located on the outside of the {Mo<sub>154</sub>} ring. Furthermore, the maximum adsorbed amount of H<sub>2</sub>O molecules also supports our suggestion. This idea can be expanded further by considering that the inner volume of the {Mo<sub>154</sub>} ring calculated from the inner diameter and the height is about 4.1 nm<sup>3</sup>, while up to 150 H<sub>2</sub>O molecules can be adsorbed per {Mo<sub>154</sub>} ring. Considering the liquid density of H<sub>2</sub>O, the adsorbed H<sub>2</sub>O molecules occupy a volume of about 4.5 nm<sup>3</sup>, which is similar to the inner volume of the {Mo<sub>154</sub>} ring. Further, the amount of H<sub>2</sub>O adsorbed by **2** is significantly lower than the amount in as-synthesized **1** (ca. 470). In the case of as-synthesized **1**, a large amount of H<sub>2</sub>O is located on the outside of the {Mo<sub>154</sub>} ring, while the outer space of **2** is occupied by alkyl chains of DODA cations, which decrease the amount of H<sub>2</sub>O adsorbed by **2**. Considering the high hydrophilicity of H<sub>2</sub>O, it can be concluded that the inner space is largely filled with H<sub>2</sub>O molecules, and the outer surface is covered by the DODA cations.

To confirm the presence of the nanospace after removal of all H<sub>2</sub>O molecules, gas and vapor adsorption isotherms were measured on samples that had been dried at 353 K under vacuum. Figure 1 shows the adsorption isotherms of N<sub>2</sub> and CO<sub>2</sub> at 77 and 195 K. Dehydrated “unprotected” **1** shows no adsorption of N<sub>2</sub> and CO<sub>2</sub> over the entire pressure range, and this indicates that dehydrated **1** has no accessible space for these gases. In contrast, the adsorption isotherms of desolvated “protected” **2** show gradual uptake, that is, dehydrated **2** has a permanent and accessible nanospace. The adsorption isotherms of H<sub>2</sub>O, MeCN, and benzene for dehydrated **2** at 298 K (Figure 2) also show gradual uptake by the nanospace.

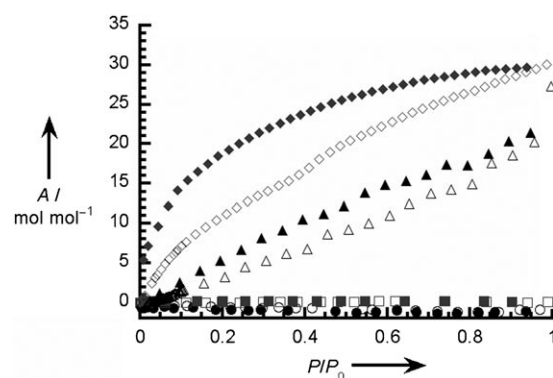


**Figure 1.** Adsorption isotherms of N<sub>2</sub> and CO<sub>2</sub> in dehydrated **1** (N<sub>2</sub>: circles, CO<sub>2</sub>: squares) and **2** (N<sub>2</sub>: triangles, CO<sub>2</sub>: diamonds) at 77 and 195 K (adsorption: empty symbols, desorption: filled symbols).

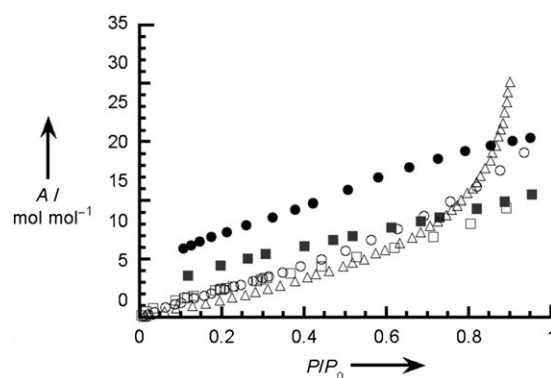


**Figure 2.** Adsorption isotherms of H<sub>2</sub>O (circles), MeCN (squares), and benzene (triangles) in dehydrated **2** at 298 K (adsorption: empty symbols, desorption: filled symbols).

All isotherms for dehydrated **2** show a gradual increase in the amount of gas adsorbed. In addition, the higher the measurement temperature is, the more the adsorbed amount increases. These results support that the gases and vapors diffuse into densely aggregated alkyl chains of DODA cations with structural transformations, that is, positional displacements of alkyl chains. The fact that the hydrophilic H<sub>2</sub>O, hydrophobic benzene, and medium-polarity MeCN are all adsorbed by dehydrated **2** indicates coexistence of a hydrophilic nanospace formed inside the {Mo<sub>154</sub>} ring and hydrophobic nanospace existing inside the aggregated alkyl chains.

Infrared spectra of pyridine-loaded **2** (Figure 3) were measured to explore the presence of Lewis and Brønsted acidic sites inside the {Mo<sub>154</sub>} ring. The positions of in-plane vibration bands of a pyridine ring strongly depend on its binding state.<sup>[12]</sup> The bands at 1539 and 1456 cm<sup>-1</sup> are attributed to pyridine adsorbed on Brønsted and Lewis acidic site, respectively, and a band at 1442 cm<sup>-1</sup>, derived from hydrogen-bonded pyridine, is also observed. Because of the high affinity for H<sub>2</sub>O molecules, H<sub>2</sub>O molecules are easily adsorbed by **2** during the handling of dehydrated **2** in the atmosphere, which was confirmed by TG and IR measurements (see Figures S6 and S11, Supporting Information).

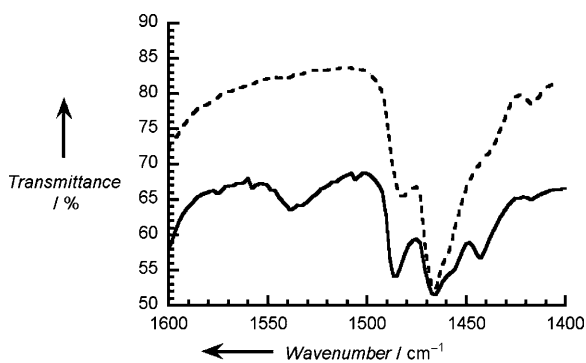


**Figure 3.** IR spectra of pyridine-loaded **2** (solid line) and **2** (dashed line).

Therefore, it can be concluded that dehydrated **2** has both Lewis and Brønsted acid sites on the inner surface of the  $\{\text{Mo}_{154}\}$  ring. Adsorption of pyridine at acid sites of the  $\{\text{Mo}_{154}\}$  ring clearly supports that the inner nanospace is accessible for guests. To our knowledge, this is the first time that a ring-shaped POM has been demonstrated to have an open, stable, and accessible nanospace after removal of all the  $\text{H}_2\text{O}$  molecules.

Protection by DODA cations makes **2** insoluble in  $\text{H}_2\text{O}$ , so we hypothesized that **2** may be a potential water-tolerant acid catalyst that is environmentally friendly with respect to corrosiveness, safety, waste generation, ease of separation, and recovery.<sup>[13]</sup> To investigate this, hydrolysis of ethyl acetate in the presence of excess water, which is a useful standard reaction for investigating water-tolerant solid acid catalysts, was preliminarily performed with **2** as catalyst. The conversion after 1 h was about 6.4%, comparable with those of  $\text{Cs}_{2.5}\text{H}_{0.5}\text{PW}_{12}\text{O}_{40}$  (ca. 6%) and H-ZSM-5 zeolite (ca. 5%), which are typical water-tolerant solid acids.<sup>[13d]</sup> No by-product was observed and these results indicate that **2** has high potential as a water-tolerant acid catalyst.

In conclusion, we have succeeded in stabilizing ring-shaped POM–DODA hybrid **2** in the solid state. Our studies have demonstrated, for the first time, that it is possible to utilize the  $\{\text{Mo}_{154}\}$  big-wheel species as a functional nanospace and stabilize the dehydrated form; lack of stability has been a major stumbling block for wider application of these species until now. Further, we showed that hybrid **2** not only has adsorption properties for gases and vapors but also high-performance water-tolerant catalytic properties, comparable to those of  $\text{Cs}_{2.5}\text{H}_{0.5}\text{PW}_{12}\text{O}_{40}$  and H-ZSM-5 zeolite, which are well-known strong acid catalysts. In future work we will investigate the self-assembly of **2** into a range of phases (including a tubular phase) using cation control, as well an expanded study to explore the catalytic properties of **2** in more detail.

### Experimental Section

**2:** A blue solution of **1** (600 mg,  $1.94 \times 10^{-2}$  mmol) in  $\text{H}_2\text{O}$  (15 mL) and a colorless solution of DODA·Cl (273 mg,  $4.65 \times 10^{-1}$  mmol) in  $\text{CHCl}_3$  (15 mL) were mixed together and stirred for 1 h. The organic phase was separated and allowed to stand overnight. After evapo-

ration of organic solvents, the residue was recrystallized from  $\text{CHCl}_3/\text{EtOH}$  (15/15 mL). The absence of  $\text{Cl}^-$  anions was confirmed by elemental analysis. Elemental analysis of **2** ( $(\text{DODA})_{23}[\text{Mo}_{154}\text{O}_{462}\text{H}_3] \cdot 70\text{H}_2\text{O}$ ) calcd (%) for  $\text{C}_{874}\text{H}_{1985}\text{Mo}_{154}\text{N}_{23}\text{O}_{532}$ : C 29.07, H 5.54, N 0.89, Cl 0; found: C 29.28, H 5.43, N 1.00, Cl 0. The quantity of adsorbed  $\text{H}_2\text{O}$  molecules in **2** was checked by thermogravimetric analysis.

Physical measurements: Dynamic light scattering was measured with an Otsuka Electronics FPAR-1000 in THF solution at 298 K. Thermogravimetric analyses and differential thermal analyses were performed with a Rigaku Thermo plus TG8120 apparatus in the temperature range between 298 and 773 K in a  $\text{N}_2$  atmosphere and at a heating rate of  $10 \text{ K min}^{-1}$ . XRD data of powder samples were collected on a Rigaku RINT-Ultima III diffractometer with  $\text{Cu}_{\text{K}\alpha}$  radiation. The adsorption isotherms for  $\text{N}_2$  and  $\text{CO}_2$ , and benzene were measured with BELSORP-max volumetric adsorption equipment. The adsorption isotherms for  $\text{H}_2\text{O}$  and MeCN were measured with BELSORP-18 volumetric adsorption equipment. The IR spectra were measured on a Perkin-Elmer Spectrum 2000 with samples prepared as KBr pellets. A high-temperature transmission cell, HT-32 (Thermo Spectra-Tech), was used to measure the temperature dependence of the IR spectra.

Pyridine-loaded **2** was prepared as follows: After heating **2** at 353 K under vacuum for 4 h, the dehydrated **2** obtained was exposed to anhydrous pyridine (Wako Pure Chemicals) for 1 h and then dried at room temperature under vacuum for 2 h.

Hydrolysis of ethyl acetate was carried out in an ampoule ( $10 \text{ cm}^3$ ) at 333 K with a 5 wt% aqueous solution of ethyl acetate ( $3 \text{ cm}^3$ , 1.7 mmol of ethyl acetate). The weight of catalyst used was 80 mg. The reactants were commercial-grade reagents (Wako Pure Chemicals) and were used as received. All solutions were prepared from Milli-Q ultrapure water (Millipore). Products were analyzed with a gas chromatograph (Shimadzu GC-14B, FID) equipped with a ZB-WAX column.

Received: June 11, 2009

Revised: July 30, 2009

Published online: October 12, 2009

**Keywords:** adsorption · heterogeneous catalysis · microporous materials · organic–inorganic hybrid composites · polyoxometalates

- [1] J. W. Patrick, *Porosity in Carbons: Characterization and Applications*, Edward Arnold, London, **1995**.
- [2] a) D. W. Breck, *Zeolite Molecular Sieves: Structure, Chemistry, and Use*, Wiley, New York, **1974**; b) S. M. Kuznicki, V. A. Bell, S. Nair, H. W. Hillhouse, R. M. Jacobinas, C. M. Braunbarth, B. H. Toby, M. Tsapatsis, *Nature* **2001**, *412*, 720–724; c) M. Sadakane, K. Kodato, T. Kuranishi, Y. Nodasaka, K. Sugawara, N. Sakaguchi, T. Nagai, Y. Matsui, W. Ueda, *Angew. Chem.* **2008**, *120*, 2527–2530; *Angew. Chem. Int. Ed.* **2008**, *47*, 2493–2496; d) A. K. Cheetham, G. Férey, T. Loiseau, *Angew. Chem.* **1999**, *111*, 3466–3492; *Angew. Chem. Int. Ed.* **1999**, *38*, 3268–3292, and references therein.
- [3] a) G. Férey, *Chem. Soc. Rev.* **2008**, *37*, 191–214; b) O. M. Yaghi, M. O’Keeffe, N. W. Ockwig, H. K. Chae, M. Eddaoudi, J. Kim, *Nature* **2003**, *423*, 705–714; c) S. Kitagawa, R. Kitaura, S. Noro, *Angew. Chem.* **2004**, *116*, 2388–2430; *Angew. Chem. Int. Ed.* **2004**, *43*, 2334–2375; d) D. Bradshaw, J. B. Claridge, E. J. Cussen, T. J. Prior, M. J. Rosseinsky, *Acc. Chem. Res.* **2005**, *38*, 273–282; e) S. Noro, S. Kitagawa, T. Akutagawa, T. Nakamura, *Prog. Polym. Sci.* **2009**, *34*, 240–279.
- [4] a) T. Ito, K. Inumaru, M. Misono, *J. Phys. Chem. B* **1997**, *101*, 9958–9963; b) N. Mizuno, M. Misono, *Chem. Lett.* **1987**, 967–

- 970; c) T. Okuhara, H. Watanabe, T. Nishimura, K. Inumaru, M. Misono, *Chem. Mater.* **2000**, *12*, 2230–2238.
- [5] a) A. Müller, E. Krickemeyer, J. Meyer, H. Bögge, F. Peters, W. Plass, E. Diemann, S. Dillinger, F. Nonnenbruch, M. Randerath, C. Menke, *Angew. Chem.* **1995**, *107*, 2293–2295; *Angew. Chem. Int. Ed. Engl.* **1995**, *34*, 2122–2124; b) A. Müller, S. K. Das, E. Krickemeyer, C. Kuhlmann in *Inorganic Syntheses* (Ed.: J. R. Shapley), Wiley, New York, **2004**, pp. 191–200; c) A. Müller, S. K. Das, V. P. Fedin, E. Krickemeyer, C. Beugholt, H. Bögge, M. Schmidtman, B. Hauptfleisch, *Z. Allg. Anorg. Chem.* **1999**, *625*, 1187–1192; d) The formula of **1** contains the reactive anion referred to in the present investigation, while in refs. [5b] and [5c] the anion with the defect is additionally mentioned as a constituent of **1**; for details, see A. Müller, C. Serain, *Acc. Chem. Res.* **2000**, *33*, 2–10; e) A. Müller, E. Krickemeyer, H. Bögge, M. Schmidtman, C. Beugholt, S. K. Das, F. Peters, *Chem. Eur. J.* **1999**, *5*, 1496–1502; f) A. Müller, F. Peters, M. T. Pope, D. Gatteschi, *Chem. Rev.* **1998**, *98*, 239–271; g) T. Yamase, P. Prokop, Y. Arai, *J. Mol. Struct.* **2003**, *656*, 107–117; h) A. Müller, M. Koop, H. Bögge, M. Schmidtman, C. Beugholt, *Chem. Commun.* **1998**, 1501–1502; i) A. Tsuda, E. Hirahara, Y.-S. Kim, H. Tanaka, T. Kawai, T. Aida, *Angew. Chem.* **2004**, *116*, 6487–6491; *Angew. Chem. Int. Ed.* **2004**, *43*, 6327–6331; j) M. A. Alam, Y.-S. Kim, S. Ogawa, A. Tsuda, N. Ishii, T. Aida, *Angew. Chem.* **2008**, *120*, 2100–2103; *Angew. Chem. Int. Ed.* **2008**, *47*, 2070–2073.
- [6] a) S. Uchida, N. Mizuno, *Coord. Chem. Rev.* **2007**, *251*, 2537–2546; b) D. Hagrman, P. J. Hagrman, J. Zubieta, *Angew. Chem.* **1999**, *111*, 3359–3363; *Angew. Chem. Int. Ed.* **1999**, *38*, 3165–3168; c) Y. Ishii, Y. Takenaka, K. Konishi, *Angew. Chem.* **2004**, *116*, 2756–2759; *Angew. Chem. Int. Ed.* **2004**, *43*, 2702–2705; d) H.-Y. An, E.-B. Wang, D.-R. Xiao, Y.-G. Li, Z.-M. Su, L. Xu, *Angew. Chem.* **2006**, *118*, 918–922; *Angew. Chem. Int. Ed.* **2006**, *45*, 904–908; e) S. S. Mal, U. Kortz, *Angew. Chem.* **2005**, *117*, 3843–3846; *Angew. Chem. Int. Ed.* **2005**, *44*, 3777–3780; f) C. Streb, C. Ritchie, D.-L. Long, P. Kögerler, L. Cronin, *Angew. Chem.* **2007**, *119*, 7723–7726; *Angew. Chem. Int. Ed.* **2007**, *46*, 7579–7582.
- [7] The size was measured by considering van der Waals radii for constituting atoms.
- [8] The replacement of inner H<sub>2</sub>O guests by other organic molecules in ring-shaped POMs have been reported.<sup>[5e,i,j]</sup>
- [9] T. Akutagawa, R. Jin, R. Tunashima, S. Noro, L. Cronin, T. Nakamura, *Langmuir* **2008**, *24*, 231–238.
- [10] a) M. Clemente-León, B. Agricole, C. Mingotaud, C. Mingotaud, C. J. Gómez-García, E. Coronado, P. Delhaès, *Langmuir* **1997**, *13*, 2340–2347; b) M. Clemente-León, C. Mingotaud, B. Agricole, C. J. Gómez-García, E. Coronado, P. Delhaès, *Angew. Chem.* **1997**, *109*, 1143–1145; *Angew. Chem. Int. Ed. Engl.* **1997**, *36*, 1114–1116; c) M. Clemente-León, T. Ito, H. Yashiro, T. Yamase, *Chem. Mater.* **2007**, *19*, 2589–2594; d) D. Volkmer, A. D. Chesne, D. G. Kurth, H. Schnablegger, P. Lehmann, M. J. Koop, A. Müller, *J. Am. Chem. Soc.* **2000**, *122*, 1995–1998; e) M. Nyman, D. Ingersoll, S. Singh, F. Bohomme, T. M. Alam, C. J. Brinker, M. A. Rodrigues, *Chem. Mater.* **2005**, *17*, 2885–2895; f) S. Liu, H. Möhwald, D. Volkmer, D. G. Kurth, *Langmuir* **2006**, *22*, 1949–1951.
- [11] In our previous report,<sup>[9]</sup> the chemical formula of **2** ((DODA)<sub>20</sub>[Mo<sub>154</sub>O<sub>462</sub>H<sub>8</sub>(H<sub>2</sub>O)<sub>70</sub>]<sub>20</sub>H<sub>2</sub>O) was determined by thermogravimetric analysis and surface area at the air/water interface. In this work, we checked the chemical formula by elemental analysis, which afforded the tentative formula (DODA)<sub>23</sub>[Mo<sub>154</sub>O<sub>462</sub>H<sub>5</sub>]<sub>70</sub>H<sub>2</sub>O. It is very difficult to determine the exact chemical formula of hybrids of DODA cations and POMs. For example, the hybrid of DODA cations and ball-shaped {Mo<sub>132</sub>} clusters afforded a margin of error for the DODA/NH<sub>4</sub> cation ratio of (DODA)<sub>40</sub>(NH<sub>4</sub>)<sub>2</sub>[Mo<sub>132</sub>O<sub>372</sub>(CH<sub>3</sub>COO)<sub>30</sub>(H<sub>2</sub>O)<sub>72</sub>]<sub>50</sub>H<sub>2</sub>O in the range of 38:4 to 42:0,<sup>[10d]</sup> which was checked by elemental analysis. Therefore, it seems that **2** also has a range of compositions regarding DODA content. In this work, we used the chemical formula (DODA)<sub>23</sub>[Mo<sub>154</sub>O<sub>462</sub>H<sub>5</sub>]<sub>70</sub>H<sub>2</sub>O determined from the elemental analysis.
- [12] a) J. W. Ward, *J. Catal.* **1967**, *9*, 225–236; b) M. R. Basila, T. R. Kantner, K. H. Rhee, *J. Phys. Chem.* **1964**, *68*, 3197–3207; c) E. P. Parry, *J. Catal.* **1963**, *2*, 371–379; d) T. R. Hughes, H. M. White, *J. Phys. Chem.* **1967**, *71*, 2192–2201.
- [13] a) T. Okuhara, *Chem. Rev.* **2002**, *102*, 3641–3666; b) N. Horita, M. Yoshimune, Y. Kamiya, T. Okuhara, *Chem. Lett.* **2005**, *34*, 1376–1377; c) H. Ishida, *Catal. Surv. Jpn.* **1997**, *1*, 241–246; d) M. Kimura, T. Nakato, T. Okuhara, *Appl. Catal. A* **1997**, *165*, 227–240.